PATENT
Docket No. 532512000500

CERTIFICATE OF MAILING BY "FIRST CLASS MAIL"

I hereby certify that this correspondence is being deposited with the United States Postal Service as first class mail in an envelope addressed to: Mail Stop Appeal Brief – Patents, Commissioner for Patents, Alexandria, VA 22313-1450, on June 7, 2005.

(Marian Christopher)

IN THE UNITED STATES PATENT AND TRADEMARK OFFICE
BEFORE THE BOARD OF PATENT APPEALS AND INTERFERENCES

In re Patent Application of:

Gregory M. LANZA, *et al.*

Serial No.: 09/774,278

Filing Date: January 30, 2001

For: ENHANCED ULTRASOUND DETECTION WITH TEMPERATURE-DEPENDENT CONTRAST AGENTS

Examiner: S. Sharareh

Group Art Unit: 1617

BRIEF ON APPEAL

Mail Stop Appeal Brief - Patents
Commissioner for Patents
P.O. Box 1450
Alexandria, VA 22313-1450

Dear Sir:

Applicants file this Brief on Appeal in regard to the rejection of claims 1, 3, 7-8, 13, 17-18, 21, 25-26, 31, 35 and 68-77, all claims pending in the above-referenced application. This Brief, along with the Appendix, is filed along with the required fee. A Notice of Appeal was filed in this action on 9 March 2005, thus setting a date for filing of the Brief of 9 May 2005. A petition for an extension of time of one (1) month until 9 June 2005 is attached along with the required fee. Appellants respectfully request reversal of the Examiner's rejection.

1. Real Party in Interest

The parties having an interest in the present invention are the assignee Barnes-Jewish Hospital having an address in Saint Louis, Missouri, and the exclusive licensee of the hospital, Kereos, Inc., also having an address in Saint Louis, Missouri.

2. Related Appeals and Interferences

To appellants' knowledge, there are no other appeals or interferences known to them or to their legal representative or assignee (or licensee) that will directly affect or be directly affected by or have a bearing on the Board's decision in the present appeal.

3. Status of Claims

The application was filed with claims 1-67.

In a response to a first Office action, claims 36-67 were canceled as directed to a non-elected invention. Claims 2, 4-6, 9-12, 20, 22-24 and 27-30 were also canceled, and all pending claims, except claims 14 and 32 were amended. Claims 68-71 were added.

In response to a subsequent Office action, claims 14-16 and 32-34 were canceled and pending claims 1, 7, 13, 17-19, 25, 31, 35, 69 and 71 were amended. Claims 72-77 were added.

In response to a final rejection, claims 1 and 18 were amended. The amendment was entered following a Request for Continued Examination (RCE).

In response to a first Office action after the RCE, claims 1 and 18 were amended. Thus, as the claims presently stand, claims 1, 3, 7-8, 13, 17-18, 21, 25-26, 31 and 35 as well as claims 68-77 are pending and on appeal; all remaining claims, claims 2, 4-6, 9-12, 14-16, 19-20, 22-24, 27-30, 32-34 and 36-67, have been canceled, as shown in the appendix.

4. Status of Amendments

Clarifying amendments were proposed in response to the final rejection, and were not entered.

5. Summary of Claimed Subject Matter

The subject matter claimed relates to the observation that liquid, non-gaseous ultrasound contrast agents provide enhanced images when the temperature is altered. This is the suggested purpose of the invention as set forth on page 3:

> None of these earlier studies disclosed or suggested changing temperature of a ultrasound contrast agent which remains in the liquid state or using the change in temperature of a non-gaseous contrast agent as a basis for enhancing ultrasound detection.

The summary of the invention on page 3, beginning at line 25, makes a further statement in this regard stating that the change of temperature of nanoparticles that contain essentially only non-gaseous fluorocarbon liquid and bound to a target results in detectable changes in acoustic reflectivity of the target.

Alternative, and substantially equivalent articulations of the invention as claimed are found on page 4 at lines 4-24.

Only minor amounts of gas are permitted to exist in the particles as set forth on page 8 at lines 17-24.

Particularly relevant to the claims is the demonstration in Examples 4 and 5 (Figures 2, 3 and 5) that an increase in temperature enhances the image of the target to which the nanoparticles are bound.

Support for claims 3, 8, 17, 21, 26 and 35 is found in the claims as originally filed.

Support for claims 7 and 25 which describe the nanoparticles as comprising at least one perfluorocarbon encapsulated with one lipid surfactant and comprising at least one ligand that

binds to the target is found, for example, on page 8, lines 6-16, with regard to the inclusion of perfluorocarbon, and on page 8, lines 25-30, for encapsulation with lipid/surfactant specifically as included in the emulsions as set forth on page 10, lines 5-10. Support for the inclusion of a targeting ligand is found, for example, on page 12, beginning at line 30, *et seq*. Support for claims 13 and 31, which describe the manner of raising the temperature, is found on page 5, lines 5-9. Support for new claims 68-71 is found in claims 5 and 23 as originally filed. Claims 72-75 are supported, for example, by original claim 16, and Examples 7 and 8.

Claims 76-77 are supported by current claims 7 and 25.

The dependent claims will not be argued separately.

6. Grounds of Rejection to be Reviewed on Appeal

Claims 1, 7-8, 13, 17-18, 25-26, 31, 35, 68-72, 74 and 76-77 are rejected as assertedly anticipated under 35 U.S.C. § 102(e) by Østenson, U.S. patent 6,375,931.

Alternatively, all pending claims are rejected as assertedly obvious over Østenson.

7. Argument

A. The pending claims are not anticipated because the particles of the invention are liquid and those of Østenson must contain gas.

Appellants' invention lies in the unexpected discovery that the imaging capability of liquid nanoparticles can be modulated by temperature. All of the claims pending are directed to methods, and both independent claims (1 and 18) make clear that the nanoparticles are liquid during the process. Aside from the fact that Østenson makes no suggestion that such a modulation of imaging capability would occur with a change in temperature of liquid nanoparticles, Østenson does not disclose any methods at all that involve liquid nanoparticles. Østenson is concerned with the behavior of gas microbubbles.

In the two independent claims on appeal, claims 1 and 18, the nanoparticles used for imaging are uniformly characterized as "liquid nanoparticles." Claim 1 involves steps (a) through (d), in each step, "liquid nanoparticles" are specified. Therefore, the statement made by the Examiner in the context of final rejection, on page 4, "The instant step (b)-(d) does not exclude formation of a gas within the particles" is simply not true. Applicants have made clear throughout the prosecution that their particles are liquid, and do not contain gas. In claim 18, which is directed to a method for obtaining an image, the step of changing the temperature of "liquid nanoparticles" specifies liquidity, and the step of obtaining an ultrasound image of the target also explicitly specifies "liquid nanoparticles." Although the substance of this claim appears to be ignored by the Examiner in the context of the final rejection, the explicit specification of "liquid nanoparticles" appears in this claim at all stages of the method as well as in claim 1.

The fact that the methods claimed by appellants require liquid nanoparticles at all times clearly distinguishes them from the processes described by Østenson which only work, according to Østenson, because gas bubbles are formed. The Examiner appears to acknowledge this on page 5 of the final rejection in the last sentence where the Examiner says:

> As described by Østenson, this steady rise of resonance intensity is attributed to an increase in microbubble size which is respectively caused by an increase in the temperature of at least 5°C of the perfluorocarbon liquid within the microbubbles of Østenson.

While this statement is not exactly accurate, since microbubble size would not be caused by any effect of temperature on a perfluorocarbon liquid, at least it is acknowledged that it is the change in the bubble's size that accounts for the enhanced reflectivity.

Østenson is quite explicit on the point that it is the increase in the size of the gas bubble that enhances the image. In column 1 it is stated:

> The present invention is based on the finding that ultrasonic visualization in a subject . . . may be achieved and/or enhanced by means of gas-containing contrast agent preparations which promote controllable and temporary growth of gas phase *in vivo* following administration.

Thus, there seems to be no dispute that the Østenson disclosure concerns gas contrast agents. But the Examiner takes the position that because the compositions may have some liquid at some time they therefore anticipate the present invention which involves liquid nanoparticles which are entirely liquid at all times.

The Examiner asserts that Østenson discloses methods of ultrasound imaging using perfluorocarbon emulsions using perfluoropentane, perfluorohexane and even perfluorooctane, some of which are used by appellants.* These are found at the cited section in column 8, which contains a long list of materials which can be used as the "diffusible component." But the diffusible component is used *in addition* to the gas dispersion. As will be made clear below, the diffusible component, even if supplied as a liquid, must, in effect, generate a gas. For example, as set forth in column 8, lines 1-10, if a water-imissible diffusible component is formulated as an emulsion, the vapor pressure in the aqueous phase of the diffusible component will be

---

* There seems to be some confusion as to the behavior of perfluorobutane. While not directly relevant to the arguments above, it should be noted that in an Office action mailed 9 March 2004, the Examiner asserted, on page 5, that perfluorobutane, among other perfluorocarbons, was a liquid at room temperature, despite the disclosure of Østenson itself that perfluorobutane is in fact a gas at 9°C. In response to applicants pointing this discrepancy out in the subsequent response, the Examiner offered the view that 9°C was not room temperature. Appellants are not aware of any liquids that recondense to liquids at temperatures higher than those at which they are in the gas phase, assuming equivalent pressure.

substantially equal to that of pure component material even in dilute emulsions. Thus, appreciable vapor pressure, equivalent to a gas, can be achieved.

B. The claims cannot be obvious over Østenson since Østenson does not teach anything about the behavior of liquid nanoparticles or the effect of temperature on imaging.

A review of Østenson makes clear that the observed change in reflectivity in ultrasound imaging is due to the gaseous nature of the contrast agent. The invention of Østenson is summarized in column 2 which describes the compositions as comprising:

> an injectable aqueous medium having gas dispersed therein and
>
> a composition comprising a diffusible component capable of diffusion *in vivo* into the dispersed gas so as at least transiently to increase the size thereof.

The Examiner is correct that the diffusible component may start out as a liquid. However, the function of the diffusible component is to increase the size of the gas bubble. It can only do this because it is, itself, a gas precursor. As stated in column 9, lines 53-55:

> It will be appreciated that in such systems it is the ultimately generated gas which is the actual diffusible component.

The temperature manipulation is designed to ensure this. As stated in the subsequent paragraph:

> In order to ensure maximum volatilization of the diffusible component following administration and to enhance growth of the dispersed gas, both of which are endothermic processes, it may be advantageous to manipulate the temperature of the solution or suspension of the diffusible component and/or the gas dispersion prior to administration and/or to incorporate exothermically reactive constituents therein; the use of such constituents which react exothermically under the influence of ultrasound radiation may be particularly advantageous.

A review of the examples set forth in Østenson verifies that no temperature change is disclosed as associated with the imaging process. The apparent belief by the Examiner that

"continuous exposure to ultrasound energy during an ultrasound imaging procedure inherently raises local temperature" seems unsupported by the cited portion of Østenson at column 5, lines 5-46. This was pointed out in the response to the final rejection, and is undisputed on the record. And the interpretation by Østenson itself is quite different; as set forth in column 12, beginning at line 59:

> Whilst we do not wish to be bound by theoretical considerations it may be that ultrasonication at least transiently modifies the permeability of the encapsulating material, the diffusibility of the diffusible component in the surrounding liquid phase and/or the frequency of collisions between emulsion droplets and the encapsulated microbubbles.

No mention of temperature rise.

There thus appears to be no disclosure in Østenson concerning the effect of temperature on enhancing ultrasound image, and Østenson's disclosure of ultrasound image enhancement relies on the expansion of gas bubbles due to the supply of a diffusible component which can itself become a gas. The present invention, on the other hand, observes a change in reflectivity due to change in temperature in the context of an entirely liquid system, a system not disclosed for any purpose by Østenson.

In summary, Østenson is directed to a method to enhance ultrasound image by expanding gas bubbles. The expansion is achieved through supplying a diffusible component which effects the expansion, presumably by virtue of its own vapor pressure. There is no discussion of any influence of temperature on the size of the bubbles (although one might expect that increasing temperature would itself increase their size) and there is no disclosure that the ultrasound itself effects an increase in temperature. The independent claims in the present application require a deliberate increase in temperature of nanoparticles that remain liquid throughout the procedure and comparing images at at least two temperatures. The claimed method is one to enhance the

reflectivity and therefore the image of a targeted material by changing the temperature to which the liquid nanoparticles bound to the target are subjected. None of this is even remotely disclosed in Østenson.†

The distinctions between the present invention and Østenson have been set forth in detail above. It should be evident that Østenson makes no suggestion to use nanoparticles that are entirely liquid in any context, much less in the invention claimed. Clearly there is no expectation based on Østenson that liquid nanoparticles would alter their reflectivity upon change in temperature, if for no other reason than any change in reflectivity described by Østenson is due to change in size of a gas microbubble, a phenomenon that cannot occur in the presently claimed methods.

8. Claims Appendix

An Appendix containing a copy of the claims as currently pending is attached.

9. Evidence Appendix

Attached hereto for the convenience of the Board as Exhibit A is a copy of an article made of record demonstrating the differences in behavior of ultrasound contrast agents based on

---

† One minor point deserves mention – Østenson describes microbubbles and the particles in the present claims are nanoparticles. The citation by the Examiner to the specification at page 21, lines 7-10, which states that useful emulsions may have nominal particle diameters from 0.01 μ-10 μ ignores the fact that the *claims* are directed to nanoparticles, and the cited section mentions particles in general, not nanoparticles. The meaning of nanoparticles is understood in the art. For example, in an article entitled "Nanomaterials in Analytical Chemistry," *Analytical Chemistry News & Features* (1998) pages 322-327a contains a definition which, concededly says that there is no universally agreed-upon definition of when a small particle qualifies as a nanoparticle. However, the document goes on: "In our research group we consider particles with at least one dimension less than 100 nm as a nanoparticle and particles with dimensions in the range of 100 nm to 10 μ as microparticles." It would not make any sense to classify micron-size particles as nanoparticles.

gas *versus* those based on liquid emulsions. The explanation of relevance on pp 6-7 of the response filed 21 January 2005 is also attached as Exhibit B.

10. Related Proceedings Appendix

Not applicable.

The Assistant Commissioner is hereby authorized to charge any additional fees under 37 C.F.R. § 1.17 that may be required by this Brief, or to credit any overpayment, to **Deposit Account No. 03-1952**.

Respectfully submitted,

Dated: June 07, 2005 By: _____

Kate H. Murashige Gregory Einhorn
Registration No. 29,959 38,440

Morrison & Foerster LLP
3811 Valley Centre Drive
Suite 500
San Diego, California 92130-2332
Telephone: (858) 720-5112
Facsimile: (858) 720-5125

APPENDIX

1. (previously presented): A method for comparing acoustic reflectivity of a target for ultrasound imaging at a lower and a higher temperature, the method comprising

(a) measuring reflectivity prior to raising the temperature of liquid nanoparticles bound to a target;

(b) raising the temperature of the liquid nanoparticles bound to said target sufficiently to produce a measurable enhancement in acoustic reflectivity of the target;

(c) measuring reflectivity after raising the temperature of the bound liquid nanoparticles; and

(d) determining the change in reflectivity of the bound liquid nanoparticles after raising the temperature compared to reflectivity prior to raising the temperature,

wherein said nanoparticles comprise at least one fluorocarbon,

said nanoparticles having been administered to said target in a non-gaseous emulsion.

2. (canceled)

3. (previously presented): The method according to claim 1 wherein the fluorocarbon is perfluorooctane.

4-6. (canceled)

7. (previously presented): The method according to claim 1 wherein the nanoparticles comprise at least one liquid fluorocarbon encapsulated with at least one lipid surfactant which comprises at least one ligand that binds to said target.

8. (previously presented): The method according to claim 1 wherein the emulsion further comprises a biologically active agent.

9-12. (canceled)

13. (previously presented): The method according to claim 1 wherein raising the temperature comprises providing the target with ultrasound or electromagnetic energy or a

combination thereof, sufficient to raise the temperature of said nanoparticles, so as to enhance acoustic reflectivity.

14-16. (canceled)

17. (previously presented): The method according to claim 1 wherein changing the temperature comprises changing the temperature of the bound nanoparticles by at least 5°C.

18. (previously presented): A method for obtaining an image resulting from enhanced acoustic reflectivity of a target for ultrasound imaging, the method comprising changing the temperature of liquid nanoparticles bound to said target sufficiently to produce a measurable enhancement of acoustic reflectivity of the target, and obtaining an ultrasound image of said target, bound to said liquid nanoparticles, wherein said nanoparticles comprise at least one fluorocarbon, said nanoparticles having been administered to said target in a non-gaseous emulsion.

19-20. (canceled)

21. (previously presented): The method according to claim 18 wherein the fluorocarbon is perfluorooctane.

22-24. (canceled)

25. (previously presented): The method according to claim 18 wherein the nanoparticles comprise at least one perfluorocarbon encapsulated with at least one lipid surfactant which comprises at least one ligand that binds to said target.

26. (previously presented): The method according to claim 18 wherein the emulsion further comprises a biologically active agent.

27-30. (canceled)

31. (previously presented): The method according to claim 18 wherein changing the temperature comprises providing the target with ultrasound or electromagnetic energy or a combination thereof, sufficient to raise the temperature of said nanoparticles, so as to enhance acoustic reflectivity.

32-34. (canceled)

35. (previously presented): The method according to claim 18 wherein raising the temperature comprises raising the temperature of the bound nanoparticles by at least 5°C.

36-67. (canceled)

68. (previously presented): The method according to claim 7 wherein the ligand is a polypeptide, a peptidomimetic, a polysaccharide, a lipid, or a nucleic acid.

69. (previously presented): The method according to claim 68 wherein the polypeptide is at least a portion of an antibody.

70. (previously presented): The method according to claim 25 wherein the ligand is a polypeptide, a peptidomimetic, a polysaccharide, a lipid, or a nucleic acid.

71. (previously presented): The method according to claim 70 wherein the polypeptide is at least a portion of an antibody.

72. (previously presented): The method of claim 1 wherein the target resides in a mammalian subject.

73. (previously presented): The method of claim 72 wherein said subject is human.

74. (previously presented): The method of claim 18 wherein the target resides in a mammalian subject.

75. (previously presented): The method of claim 74 wherein said subject is human.

76. (previously presented): The method of claim 1 wherein said nanoparticles comprise at least one liquid fluorocarbon encapsulated with at least one lipid surfactant.

77. (previously presented): The method of claim 18 wherein said nanoparticles comprise at least one liquid fluorocarbon encapsulated with at least one lipid surfactant.

Acoustic Characterization in Whole Blood and Plasma of Site-Targeted Nanoparticle Ultrasound Contrast Agent for Molecular Imaging

Michael S. Hughes, Jon N. Marsh,

Washington University School of Medicine, Cardiovascular Division, St. Louis, MO 63110,

Christopher S. Hall

Philips Research, USA, Briarcliff Manor, NY 10510,

Ralph W. Fuhrhop, Elizabeth K. Lacy, Gregory M. Lanza, Samuel A. Wickline,

Washington University School of Medicine, Cardiovascular Division, St. Louis, MO 63110,

Uploaded: 12/29/03

Acoustic Characterization in Whole Blood and Plasma of Site-Targeted

ABSTRACT

The ability to enhance specific molecular markers of pathology with ultrasound has been previously demonstrated by our group employing a nanoparticle contrast agent[1, 2]. One of the advantages of this agent is very low echogenicity in the blood pool that allows increased contrast between the blood pool and the bound, site-targeted agent. We measured acoustic backscatter and attenuation coefficient as a function of the contrast agent concentration, ambient pressure, peak acoustic pressure, and as an effect of duty cycle and waveform shape. Measurements were performed while the nanoparticles were suspended in either whole porcine blood or plasma. The nanoparticles were only detectable when insonified within plasma devoid of red blood cells and were shown to exhibit backscatter levels more than 30dB below the scatter from backscatter from whole blood. Attenuation of nanoparticles in whole porcine blood was not measurably different from that of whole blood alone over a range of concentrations up to 8 times the maximum in vivo dose. The resulting data provide upper bounds on blood pool attenuation coefficient and backscatter and will be needed to more precisely define levels of molecular contrast enhancement that may be obtained in vivo.

PACS numbers: 43.35.Bf, 43.80.Qf

I. INTRODUCTION

Molecular imaging promises to extend diagnostic imaging from identification of functional and morphological changes associated with pathology to the direct visualization of the biochemical disease process. To accomplish this goal, molecular imaging employs the use of specially designed contrast agents. These agents are formulated to provide contrast in the imaging modality by specifically binding to proteins expressed in the diseased tissue. By targeting specific markers of pathology, a physician may diagnose disease in its early phases and design a concomitant treatment.

In the field of ultrasonic site-targeted contrast imaging, there exist several likely candidates for contrast particles[3-6]. In particular, two distinct types of particles have been explored extensively in the last decade: microbubbles and liquid nanoparticles. Despite their different physical mechanisms of ultrasonic enhancement, they both share some of the same challenges in becoming viable and useful targeted contrast agents. Common properties of a successful contrast agent include longevity within the blood stream, low toxicity, high signal to background enhancement, and high specificity for the targeted disease process. In some applications, such as detection of tumor angiogenesis, ability to easily penetrate neovasculature is also a desirable property. Nanoparticles may enjoy a slight advantage is this application due to their smaller size. The size of the particle is also closely linked with the longevity in the blood pool before being filtered by

the liver or other clearance organs, and therefore the smaller agents have increased likelihood of binding to the target.

High signal to background enhancement requires the ability to detect the presence of contrast when bound to the target and to differentiate it from surrounding unbound, circulating contrast agent. The current study examines the capability to differentiate liquid, perfluorocarbon nanoparticle contrast agents when bound from unbound. Previous studies from our laboratory have shown that these nanoparticles can be targeted to tissue factor expressed in injured carotid arteries, fibrin strands within non-echogenic plasma clots, and $\alpha_v\beta_3$ integrin expression in neovasculature surrounding a growing tumor[4, 7-9]. One of the striking features of this agent is that at typical *in vivo* concentrations, the nanoparticles are not detectable in the blood stream with clinical ultrasound imagers, but only acoustically enhance a targeted substrate when they accumulate in sufficient quantity.

The rationale for this study derives from the need to differentiate the physical behavior of these liquid perfluorocarbon nanoparticles from that of the commonly used gaseous microparticles that are comprised of a much lower boiling point perfluorocarbon [6, 10]. In addition, similar agents have been posited to be a candidate for targeting in the liquid phase, and then converted to the gas phase with energy deposited by high intensity ultrasound for imaging purposes.

Accordingly, the primary goal of this study was to perform high-precision *in vitro* measurements of these parameters to determine the ultrasonic backscatter from nanoparticles in suspension at concentrations that occur *in vivo*. By characterizing the agents' backscatter relative to that from blood, future *in vivo* studies can be assured that any increase in backscatter associated with targeted tissue that occurs after delivery of the contrast agent is due solely to bound contrast.

A secondary goal of this study was to evaluate the stability of the nanoparticle emulsion in high intensity ultrasonic fields. This was accomplished by demonstrating that the primary mode of backscatter from the liquid nanoparticles was due to simple linear backscatter from a liquid sphere and not from more esoteric processes such as phase conversion of the perfluorocarbon liquid inside the nanoparticles.

II. METHODS

A. Formulations and experimental conditions investigated

The nanoparticles used in our study are spherical as shown in **Figure 1.** They contain a perfluorocarbon core (perfluorooctyl bromide (PFOB) is shown in the figure although other perfluorocarbons (PFCs) having relatively high boiling points have also been investigated) stabilized by a lipid monolayer. This is a well-known structure for perfluorocarbon-lipid emulsions.[11, 12](Figure 1 and 3a of reference [11] and Figure 23.17 and 23.18a of reference [12]).

Two different formulations of emulsion were used in our investigations. The emulsion was produced by incorporating biotinylated phosphatidylethanolamine into the emulsion's outer lipid monolayer. Briefly, the emulsion comprised perfluorocarbon ((PFOB): boiling point of 142° C, either 40% vol/vol or 20%vol/vol), safflower oil (2.0%, wt/vol), a surfactant comixture (2.0%, wt/vol), and glycerin (1.7%, wt/vol). The surfactant comixture included 70 mol% lecithin (Pharmacia Inc), 28 mol% cholesterol (Sigma Chemical Co.), and 2 mol% N-(6-(biotinoyl)amino)hexanoyl)-dipalmitoyl-L-alpha- phosphatidylethanolamine (Pierce), which were dissolved in chloroform, evaporated under reduced pressure, dried in a vacuum oven overnight at 50 °C, and dispersed into water by sonication. The suspension was transferred into a blender cup (Dynamics Corp of America) with perfluorocarbon, safflower oil, and distilled, deionized water and emulsified for 30 to 60 seconds. The emulsified mixture was transferred to an emulsifier (Microfluidics S110) and continuously processed at 20,000 psi for 3 minutes. The completed emulsion was placed in stoppered, crimp sealed vials and blanketed with nitrogen until use. Particle sizes were determined in triplicate at 37 °C with a laser-light-scatter, submicron-particle-size analyzer (Zetasizer 4, Malvern Instruments Inc., Southborough, MA). Particle size was measured at 200±30 and 250 ±30nm, respectively.

The attenuation coefficient and backscatter of the agent were measured in either: 1) whole porcine blood (hct 40%); 2) porcine plasma maintained at 37° C; or 3) in saline maintained at 27, 37, or 47° C, which were chosen to span the possible range of temperatures used in either hyper- or hypothermia. (Saline was degassed prior to use by

heating it to 47° C for at least one hour prior to use.) In addition, for the saline-based measurements, ambient pressures were varied from –50 to +200 mm Hg in 50 mm Hg steps.

For purposes of comparison we also measured the attenuation of the microbubble-based agent Optison as part of our investigation. Since the behavior of this agent is well known, these measurements provide validation of our material handling and data analysis techniques as well as the acoustic hardware component of our apparatus[13-15].

Specimens were insonified using either a broadband high power PZT single element transducer (5 MHz, 2.54 cm diameter, 5.08 cm focal length), or a lower power PVDF single element transducer (1.02 cm diameter, 7.08 cm focal length) optimized to provide broadband measurements[15](Figure 4). Together, these enabled measurements to be made using acoustic pulses with usable bandwidth of 1.5 to 10 MHz, a repetition rate of 1kHz, and peak negative pressures of 0.8, 1.5, 2.7, and 3.9MPa (equivalent to M.I. of: 0.36, 0.67, 1.2, and 1.7) to measure attenuation coefficient and backscatter of nanoparticles at concentrations ranging from 0.16 to 2.5×10^{12} particles/mL while suspended in either whole porcine blood or porcine plasma, or saline.

B. Broadband attenuation measurements

Several different electronic pulser/receiver systems were used to acquire the data described in this paper. The first system was a through-transmission system optimized to produce the broadest possible bandwidth measurement of attenuation using single-

element PVDF transducers. The benefits of using broadband single transducer system have been elucidated in previous studies [13]. Two different electronic setups were used to drive the transducer and are shown in Figure 2.

In the first setup the PVDF transducer was excited using a DC voltage step. The pulser system was composed of a function generator (model 8116A, Hewlett Packard, Palo Alto, CA), a high voltage power supply (model PS310, Stanford Research Systems, Inc., Sunnyvale, CA), and a power MOSFET switch (model GRX-1.5K-E, Directed Energy, Inc., Ft. Collins, CO). This system produced square pulse trains whose duty cycle and amplitude could be precisely controlled. For the measurements described in Figures 4 and 6, the transducer was excited on the downward sloping edge of a square pulse (1 kHz pulse repetition frequency), which yielded a broadband (0.8 to 16 MHz at -20 dB level) ultrasonic pulse. The subsequent upward sloping edge of the exciting square pulse occurred 40 μs later. The chamber's apparent back wall echo occurred less than 5 μs after the front wall echo, so that effects of the second excitation occurred significantly later, and were excluded from acquisition (this was verified by testing separations of different lengths; 40 μs was chosen because it was twice the apparent "safe" separation distance). A diplexer (model RDX2, Ritec Inc., Warwick, RI) was placed in line between the pulser and transducer for impedance matching and to protect the receiver input from the high-voltage electronic excitation pulse. A digital delay generator (model DG535, Stanford Research Systems, Sunnyvale, CA) with maximum jitter of 50 picoseconds was used to trigger the digitizer to start acquiring the waveform after a delay relative to the

initial excitation of the transducer; this delay corresponded to the ultrasonic travel time for a backscattered echo to be received by the transducer.

The radio-frequency waveform was sampled at 250 megasamples per second by an 8-bit digitizer (Compuscope 2125, Gage Applied Sciences Inc., Montreal, Canada). Five RF traces (each 2048 points long) were acquired by averaging 1000 single-shot rf traces at each concentration of contrast agent in the chamber. This acquisition rate was selected based on the approximate mixing frequency of the paddle (Fig. 2), so that each trace was acquired from a different independent spatial distribution of the scatterers. A PC (2.3 GHz Pentium 4) was used to control acquisition and to store data to disk.

A reference trace was acquired in the same fashion as for the sample traces, using a specimen chamber filled only with Isoton, to correct for reflection at the water/chamber interfaces. Immediately after each data run, the sample path length was determined ultrasonically by measuring the time interval between the through-transmitted signal and the signal from the first round-trip reverberation. The thickness determined in this manner varied between 0.23 and 0.30 cm for the measurements in this study.

The specimen chamber used for this series of measurements is shown in the panel inset of Figure 2. In all cases the sample chamber was tilted at 10° relative to the insonifying transducer to reduce front wall ringdown and was positioned so that its front surface was at the focal distance of the transducer. The suspension was mixed continuously during the course of each of these measurements by a thin plastic rod

connected to a pressure sealed handle. The chamber has four ports on its top, which may be sealed or connected via flexible plastic tubing to various fixtures for measurement and control of ambient pressure. These fixtures permitted ambient pressure to be maintained at constant levels ranging between –50 to 200 mm Hg during acoustic data acquisition.

Measurements of the attenuation coefficient were also performed by insonifying the suspensions with the waveform shown in Figure 5, which is composed of two high-power unipolar pulses preceded by 5 cycles of a 1 MHz sine wave of the same amplitude, emitted at a high repetition frequency (5 kHz). This waveform was chosen using two criteria. The first part matches closely the transmitted waveform of a medical imaging system in pulsed Doppler mode. The second part was chosen for the reasons described above: unipolar pulses are typically broader band than bipolar waveforms and hence have a greater chance of detecting microbubble-like features in the resulting backscatter or attenuation curves.

C. Backscatter measurements

The electronics used to perform backscatter measurements are shown in Figure 3. The transducer shown in the figure is a large diameter (2.54 cm dia.), highly focused (5.05 cm F.L., 5.0 MHz C.F.) PZT transducer; these parameters were chosen to obtain increased sensitivity within the focal zone and to reduce sensitivity to ringdown from front and back chamber walls. The driving electronics employ a commercial pulser/receiver (Panametrics 5800). The computer controller, digitizer and delay generator are the same as in Figure 2 and were used the same way.

During the course of measurements, 70 mL of either whole porcine blood (Hct 40%, with 5% sodium citrate solution added to prevent clotting) or plasma was added to the chamber and thoroughly mixed. The liquid was then allowed to sit unstirred and the backscatter signal from the mixture monitored until a stable equilibrium was reached. Observation of the rf signal during this time indicates the presence of many large and transient scatterers in the focal zone (perhaps spurious bubbles produced by mixing). These gradually disappear as the rate of change in signal shape rapidly decreases, until after roughly 10 minutes, the backscatter signal is only slowly changing, indicating that the blood components have reached a stable scattering configuration. The backscatter signal for plasma alone is quiescent except for the presence of electronic noise. Data were actually acquired after waiting 60 minutes in order to make sure that scatterers had reached a stable configuration. We observed that the backscatter for blood measured in this equilibrium state is at least 30dB higher (see Figure 6 and discussion in results section) than that measured immediately after introduction of the blood into the specimen chamber, which is consistent with, although greater in magnitude than, observations of other researchers performing similar investigations [16, 17]. Also, as Figure 6 will show, in the equilibrium state the backscatter from all concentrations studied is experimentally indistinguishable, indicating that the concentrations of scatterers in the focal zone of the transducer are probably the same in each case. This is a reasonable outcome given the goal of our study, which was to determine the values delimiting an upper bound on the backscatter of nanoparticles that might be observed from the blood pool *in vivo* and serve to define a useful bound on the contrast-to-background ratio that might be obtained in

clinical application at various doses. Other studies would be required to determine the concentration dependent backscatter and attenuation of nanoparticles in mixed or flowing blood or plasma. Observations from our apparatus indicate that precise measurements in these flow regimes would be practically impossible. Moreover, the value of such data for evaluation of backscatter from targeted surfaces would seem to be extremely limited; creation of measurable backscatter from smooth targeted surfaces, at least at frequencies above 25 MHz is an established fact[18, 19]. The unknown at this point is determination of backscatter from diffuse fractal-like neovascular networks associated with new tumor growth[20-23]. Determination of backscatter from these scattering configurations is an active area of research in our laboratory and will be described in a future report.

The same settling phenomenon is observed for nanoparticles mixed into either whole blood or plasma. Consequently, all measurements were made 60 minutes after introduction of nanoparticles for the reasons discussed above. As the backscatter signals are acquired when the fluid-nanoparticle mixture is relatively static, we acquire data by scanning the transducer on a 50x20 point grid of points 0.5mm apart to gather 1000 rf waveforms each of which is 8192 points long (equivalent to 16 μs) and comprised of 8-bit values. This spatial grid was chosen to provide statistically independent backscatter traces and was placed as close as possible to the bottom of the chamber, where scatterer concentration is expected to be highest, consistent with our goal of measuring the upper bounds of attenuation and backscatter that might occur *in vivo*. These waveforms are gated with a 6 μs window, Fourier transformed and the electronic response of the system is deconvolved from the backscatter data using a reference acquired from a stainless steel

plate. The results are then averaged together to compute the average apparent backscatter transfer function.

The specimen chamber used for this series of measurements is shown in the right panel of Figure 3. The chamber is comprised of three circular plates clamped together to hold two Saran Wrap films to create the sample volume denoted by the region gray in the figure. This region is 7.62 cm in diameter and 5.08 cm thick. These dimensions were chosen to create a sample volume thick enough to permit acquisition of a 6.0 μs window free from measurable ringdown from the front wall membrane. The chamber has a port on its top through which plasma, blood and/or emulsion are added. A plug on the bottom of the chamber may be removed to drain and wash the chamber. In all cases the sample chamber was positioned so that its front surface was 5 mm beyond the focal distance of the transducer, this was done so that the first point of the digitized time domain window was 8μs after the front wall ringdown. The chamber was also tilted at 10° relative to the insonifying transducer to further reduce front wall ringdown, as shown in Figure 3. The suspension was mixed using a disposable 5 mL pipette for one minute and then r.f. data acquired subsequent to a 60 settling minute period as described above.

III. RESULTS

Attenuation measurements have been obtained over a large set of experimental parameters: nanoparticle concentration, ambient pressure, ambient temperature, peak positive acoustic pressure, exposure time, and using two different waveform shapes. The

attenuation measurements were undertaken primarily to investigate the hypothesis that liquid-to-gas phase conversion of nanoparticles into microbubbles does not occur at detectable levels under *in vivo* conditions with current clinical imagers.

Backscatter results have also been made under several different conditions, the most important parameters considered for this part of the study were: nanoparticle concentration and the type of fluid in which the emulsion was mixed for the measurement. These measurements were undertaken to investigate the hypothesis that nanoparticle scattering in the blood pool is not measurable under *in vivo* conditions with current clinical imagers. Moreover, we have chosen to report the apparent backscatter, i.e., we have specifically chosen not to report backscatter compensated for attenuation. This choice was made for three reasons. First, uncompensated or apparent backscatter is the basic experimentally measured quantity describing backscatter and is consequently accessible to any experimentalist using the same transducer described above. Second, diffraction compensation requires choice of a specific field model[24-29]; a choice for which there is no universally accepted standard. Thus, the uncompensated data should have greater utility as they can be corrected according to one's favorite model using the transducer information supplied above. Third, the backscatter values obtained over all concentrations studied are essentially the same at the equilibrium described in the methods section so that, the attenuation corrected backscatters would be also, thus, rendering the correction largely academic.

The outcome of both backscatter and attenuation results are summarized in tables IA and IB.

A. Broadband attenuation measurements

The attenuation coefficient of Optison is plotted as a function of frequency in the top row of graphs of Figure 4 for three different ambient pressures: 0, 120 and 200 mm Hg (these data were acquired using the unipolar pulser apparatus described in Fig. 1 of [30]). The concentration for all of these measurements was $3.3x10^5$ microbubbles/mL, which was chosen so that the attenuation would be roughly equal to that produced by nanoparticles in the concentrations used for this study. All Optison data were acquired under the same conditions as were used to acquire the nanoparticle data also shown in Figure 4. The peak height and width and its exact location clearly depend on ambient pressure and also exposure time (ranging between 2 to 80 s for the data shown). These attenuation coefficient changes are probably the result of: 1) microbubble destruction, 2) gas exchange with the surrounding liquid medium (particularly oxygen uptake by the perfluoropropane) that results in mean microbubble diameter increase, and 3) changes in mean microbubble diameter induced by changes in ambient pressure[30, 31]. These data were acquired with an insonifying pressure of 0.65 MPa and the figure clearly shows that even at this relatively low acoustic pressure the microbubble-based agent undergoes fundamental changes in its composition resulting in dramatically variable acoustic behavior. The corresponding data obtained from the PFOB-based nanoparticle contrast agent are shown in the second row of Figure 4 (data obtained from a suspension of $2.5x10^{12}$ particles/mL in saline). It is apparent that there is no dependence on either the ambient pressure or the exposure time, nor is there any evidence of a peak in the

attenuation coefficient. All evidence strongly suggests that ultrasound-induced liquid to gas phase conversion does not significantly contribute to the acoustic performance of the PFOB emulsion.

The third and fourth rows of Figure 4 (data obtained from a suspension of 1.2×10^{12} particles/mL in saline) summarize results from measurements made with emulsions exposed to a higher insonifying acoustic pressure (peak positive and negative pressure levels of 3.0 MPa), at ambient temperatures of 37 C and 46 C, respectively. There is no dependence of the attenuation coefficient on exposure time or ambient pressure.

In Figure 5 we show the results obtained using, a preheating pulse (5 cycles of a 1 MHz sine wave burst with peak pressures of 3 MPa) to further investigate the possibility of liquid to gas phase conversion. The shape of this pulse is shown in panel A of Figure 5. The data in panel B of this figure show the attenuation coefficient of the PFOB based emulsion obtained at 37 C. These data exhibit no evidence of the resonant peak typically associated with the presence of microbubbles, which for comparison are plotted in panel C of the figure. This observation also makes it appear unlikely that liquid to gas phase conversion occurs.

B. Backscatter measurements

Figure 6 shows that the acoustic properties of the PFOB-based nanoparticle emulsion are nearly optimal for application as a site-targeted contrast enhancer. The top two panels compare the attenuation coefficient of whole porcine blood (HCT 40%) with attenuation from nanoparticles suspended in porcine plasma. The left top panel compares the attenuation from 70 mL of whole porcine blood obtained after adding 0.25, 0.5, and 1.0 mL of nanoparticle emulsion. These correspond to doses more than 8 times that which might be used clinically. In addition, at higher doses, there was noticeable precipitation of nanoparticles from the suspension. All measurements were made one hour after adding emulsion and mixing because one hour is about the time required for the nanoparticle/blood cell scatterers to come to equilibrium. In all cases studied there was no statistically significant difference between attenuation of whole blood and attenuation of blood with emulsion. This outcome is consistent with the attenuation measurement of emulsion in plasma (also post 1-hour mixing) shown in the right top panel.

The bottom two panels of Figure 6 show the corresponding apparent backscatter transfer functions (i.e. backscatter not compensated for attenuation or transducer effects). The left panel shows backscatter of whole porcine blood plotted along with backscatter from 70 mL of whole blood plus 0.25, 0.5 and 1.0 mL of emulsion (corresponding to 1.55, 3.10, and 6.19×10^{11} particles/mL respectively). The left panel again shows that the addition of emulsion produces no statistically significant alteration of backscatter relative

to that from blood (using the standard errors of each measured point as the basis for statistical significance). This is further supported by the data shown in the right bottom panel, which shows apparent backscatter (post one hour mixing) of plasma compared to plasma plus 0.25, 0.5 and 1.0 mL of emulsion. The backscatter from the plasma is different from that of the plasma plus emulsion (thus establishing that the backscatter result in whole blood is not the result of insufficient measurement sensitivity), however, all curves are more than 30dB below backscatter of whole blood. The plasma only curve also indicates the noise floor of our apparatus for backscatter measurements.

IV. Discussion

One of the desired goals for a successful, targeted contrast agent is the ability to differentiate the targeted pathology from the surrounding tissue. Often, a technical dilemma arises with the use of a highly echogenic contrast agent. The choice of high echogenicity increases the signal received back from the imaged tissue, but the ability to adequately differentiate bound from adjacent circulating unbound contrast agent can be difficult since significant concentrations of nonspecifically bound bubbles can be anticipated. Several solutions have been proposed. One simple approach includes waiting for the freely circulating particles to be cleared from the blood pool. This approach is used in targeting with other imaging modalities including nuclear imaging. The assumption is that the bound particles have sufficient longevity to survive at the targeted site until the circulating particles are gone. The clearance approach has several disadvantages including the length of time of the diagnostic imaging procedure, and the

difficulty in designing an agent with the conflicting goal of existing long enough to bind to the targeted pathology but also exhibiting rapid clearance.

A second approach has been used with some success in the targeting of microbubbles [32-34]. This approach utilizes the fact that microbubbles can be destroyed in a high intensity ultrasonic field. After waiting sufficiently long to allow binding, an image is obtained of the tissue containing bound and unbound bubbles. The tissue is then exposed to a high intensity ultrasonic wave to destroy all microbubbles. After a short time in which it is postulated that microbubbles have again entered the imaging plane but not yet had time to bind in sufficient quantities, a second image is acquired. By subtracting these two images, the bound bubbles can be visualized. Although quite successful in some studies, there are some disadvantages to this approach including misregistration of images before subtraction, a problem that may be acute in moving organs such as the heart or in patients where breathing may move the imaging plane. Another possible disadvantage is that this approach allows only one chance to image the targeted contrast agent before it is destroyed.

The nanoparticle contrast agent described in this study attempts to address the problem of differentiating bound from unbound agent by utilizing a nanoparticle with reduced blood pool echogenicity. The targeted pathology is detectable only after the nanoparticles are bound in quantity. The results displayed above show that the nanoparticle contrast agent has ultrasonic backscatter that is less than that of circulating red blood cells when administered in concentrations typical of *in vivo* use. The

nanoparticles were only detectable when insonified within plasma devoid of red blood cells and were shown to exhibit backscatter levels more than 30dB below the scatter from backscatter from red blood cells. The weak scatterer hypothesis is supported by the fact that low acoustic pressure measurements of nanoparticle emulsion show that the backscatter is not measurably different from background (i.e., measurement of backscatter from either water or plasma alone).

A second goal of these measurements was to determine the stability of the nanoparticle contrast agent in the presence of a high intensity ultrasonic field. The experiment was designed to determine whether the contrast provided by the nanoparticles was due to a conversion of the perfluorocarbon from liquid to a gaseous phase or to its own intrinsic scattering behavior in the liquid phase. To determine whether this phase conversion occurred, the nanoparticles were examined for two characteristics typically associated with gas bubbles under ultrasonic insonification. The first characteristic was the appearance of non-linear promotion of ultrasonic energy into a scattered harmonic frequency. The second characteristic was related to physical changes that might occur as a function of exposure time to ultrasound. These changes are related to the destruction of microbubbles with increasing ultrasonic intensity and exposure time. To examine the possibility of this occurrence, microbubbles (Optison) and nanoparticles were measured in a similar experimental setup.

The data in Figures 4, 5, and 6show that nanoparticle suspension attenuation coefficient is not measurably affected by changes in hydrostatic or acoustic pressure.

Moreover, the data exhibit no evidence of scattering agent destruction as the duration of ultrasound exposure increased. This observation is independent of incident acoustic pressure for both low power (0.65 MPa) unipolar pulses and high-power (3.0 MPa) unipolar pulses, which is a range of pressures spanning current clinical ultrasound application. When the same range of pressures is used to measure the attenuation coefficient of Optison, significant changes in attenuation coefficient are observed: the microbubble agent attenuation coefficient exhibits a single peak between 1 and 2 MHz, and the exact peak location, height and width vary significantly with experimental conditions. In contrast, the emulsion does not exhibit these effects.

Thus, it is unlikely that microbubble formation through perfluorocarbon phase conversion contributes in a measurable manner to the acoustic properties of the liquid perfluorocarbons nanoparticle contrast agent over the range of experimental parameters considered in this study. Such a conversion, if it were to occur, would deplete the population of nanoparticles, which would then be destroyed in the same manner observed for Optison, leading to a measurable decrease in attenuation coefficient. Furthermore, the attenuation coefficient of the nanoparticle emulsion was a linear function of frequency at all concentrations and power levels and showed no evidence of a resonant peak characteristic of liquid-to-gas phase conversion. In fact, the linearity of the attenuation data is consistent with a combination of absorption and scattering. This implies that the absorption cross section dominates the scattering cross-section during wave propagation through the emulsion [35][pg 20 Eqn. 2-32][36][pg 427, Eqn. 8.2.19]. Additionally, the attenuation is quite low, which is again consistent with our assumption of weak

scattering. The combination of these measurements strongly indicates that there is little to no phase conversion to gas of the liquid perfluorocarbon nanoparticles used in this study.

V. CONCLUSION

The attenuation coefficient of perfluorocarbon nanoparticles under a wide range of experimental conditions is linear, indicating that weak absorption is the primary scattering mechanism. No evidence of strong scattering or resonant behavior was observed over a range of conditions that certainly encompasses those expected in clinical application of ultrasound.

Moreover, attenuation and backscatter measurements from emulsion in whole blood compared to corresponding measurements in plasma indicate that, when suspended in whole blood, even relatively high concentrations of the emulsion produce no measurable changes in linear acoustic behavior of the blood pool. The resulting data provide upper bounds on blood pool acoustic parameters and more precisely define levels of molecular contrast enhancement that may be obtained *in vivo*. Low blood pool backscatter is one of the advantages of this agent as relative non-echogenicity in the blood pool allows increased contrast-to-noise between the blood pool and the bound, site-targeted agent.

We have shown that the liquid, perfluorocarbon nanoparticles provide minimal contrast when circulating the blood pool under fundamental imaging conditions. The low inherent echogenicity of the particles when in suspension is a feature that allows for

differentiation of the bound, targeted nanoparticles from those circulating freely in the body. The stability of the nanoparticles is far greater than that of microbubbles after exposure to high intensity ultrasonic fields. Future studies will measure other properties of nanoparticle contrast agents such as optimized detection of the contrast agent when bound to a substrate *in vivo*.

ACKNOWLEDGEMENTS

This work was supported in part by HL-59865 and N01-C0-07013-32.

REFERENCES

1. Lanza, G.M., et al., *Molecular imaging of stretch-induced tissue factor expression in carotid arteries with intravascular ultrasound.* Investigative Radiology, 2000. **35**(4): p. 227-234.
2. Lanza, G.M., et al., *High-frequency ultrasonic detection of thrombi with a targeted contrast system.* Ultrasound in Medicine and Biology, 1997. **23**(6): p. 863-870.
3. de Jong, N. and F.J.T. Cate, *New ultrasound contrast agents and technological innovations*, in *Ultrasonics*. 1996. p. 587-590.
4. Lanza, G., et al., *In Vitro Characterization of a Novel, Tissue-Targeted Ultrasonic Contrast System with Acoustic Microscopy*, in *Journal of the Acoustical Society of America*. 1998. p. 3665-3672.
5. Unger, E.C., et al., *In vitro studies of a new thrombus-specific ultrasound contrast agent*, in *The American Journal of Cardiology*. 1998. p. 58G-61G.
6. Cotter B., K.O.L., Kimura B., Leese P., Quay S., Worah D., Demaria A.N.,, *Evaluation of the efficacy, safety and pharmacokinetics of QW3600 (Echogen) in man.* Circulation, 1994. **90**(4): p. 555-555 part 2.
7. Lanza, G. and S. Wickline, *Targeted Ultrasonic Contrast Agents for Molecular Imaging and Therapy*, in *Progress in Cardiovascular Diseases*. 2001. p. 13-31.
8. Lanza, G., et al., *Molecular imaging of stretch-induced tissue factor in carotid arteries with ligand-targeted nanoparticles*, in *Investigative Radiology*. 2000. p. 227-234.
9. Lanza, G., et al., *In vivo molecular imaging of stretch-induced tissue factor in carotid arteries with ligand targeted nanoparticles*, in *Journal of the American Society of Echocardiography*. 2000. p. 433-439.

10. Marsh, J.N., Hall, Christopher.S., Scott, Michael.J., Fuhrhop, Ralph.W., Gaffney, Paul.J., Wickline, Samuel.A., Lanza, Gregory.M., *Improvements in the ultrasonic contrast of targeted perfluorocarbon nanoparticles using an acoustic transmission line model.* IEEE Transactions on Ultrasonics Ferroelectrics and Frequency Control, 2002. **49**(1): p. 29-38.
11. Riess, J.G. and M.P. Krafft, *Fluorocarbons and fluorosurfactants for in vivo oxygen transport (blood substitutes), imaging and drug delivery.* MRS Bulletin, 1999. **24**: p. 42-48.
12. Riess, J.G., *fluorocarbon emulsions-Designing an Efficient Shuttle service for the Respiratory Gases - The So-called "Blood Substitutes"*, in *Fluorine Chemistry at the Millennium*, R.E. Banks, Editor. 2000, Elsevier Science: Oxford, UK. p. 385-431.
13. Hughes, M.S., et al. *Comparison of Ultrasound Scattering Behavior of Optison® and a Liquid Perfluorocarbon Nanoparticle Contrast Agent.* in *2002 IEEE Ultrasonics Symposium.* 2002: IEEE.
14. Hughes, M.S., et al. *Comparison of Ultrasound Scattering Behavior of Optison and a Liquid Perfluorocarbon Nanoparticle Contrast Agent.* in *142nd Meeting Acoustical Society Of America.* 2001. Fort Lauderdale FL: AIP.
15. Marsh, J.N., et al., *Broadband through-transmission signal loss measurments of Albunex suspensions at concentrations approaching in vivo doses.* Journal of the Acoustical Society of America, 1997. **101**(2): p. 1155-1161.
16. Yuan, K.K. and K.K. Shung, *Ultrasonic backscatter from flowing whole blood. I: Dependence on shear rate and hematocrit.* Journal of the Acoustical Society of America, 1988. **84**(52): p. 52-58.
17. Wang, S.-H. and K.K. Shung, *In vivo measurements of ultrasonic backscattering in blood.* IEEE Transactions on Ultrasonics Ferroelectrics and Frequency Control, 2001. **48**(2): p. 425-431.
18. Hall, C.S., et al., *Temperature dependence of ultrasonic enhancement with a site-targeted contrast agent.* Journal of the Acoustical Society of America, 2001. **110**(3): p. 1677-1684.
19. Hall, C.S., et al., *Time evolution of enhanced ultrasonic reflection using a fibrin-targeted nanoparticulate contrast agent.* Journal of the Acoustical Society of America, 2000. **108**(6): p. 3049-3057.
20. Ahmed, E., *Fractals and Chaos in Cancer Models.* International Journal of Theoretical Physics, 1993. **32**(2): p. 353-355.
21. Beier, J., et al., *Fractal surface analysis of pulmonary nodules based on high resolution computed tomography.* Rofo-Fortschritte Auf Dem Gebiet Der Rontgenstrahlen Und Der Bildgebenden Verfahren, 1997. **166**(4): p. 296-302.
22. Baish, J.W. and R.K. Jain, *Cancer, angiogenesis and fractals.* Nature Medicine, 1998. **4**(9): p. 984-984.
23. Baish, J.W. and R.K. Jain, *Fractals and cancer.* Cancer Research, 2000. **60**(14): p. 3683-3688.
24. Sigelmann, R.A. and J.M. Reid, *Analysis and measurement of ultrasound backscattering from an ensemble of scatterers excited by sine-wave bursts.* J. Acoust. Soc. Am., 1973. **53**: p. 1353-1355.

25. O'Donnell, M. and J.G. Miller, *Quantitative broadband ultrasonic backscatter: An approach to nondestructive evaluation in acoustically inhomogeneous materials.* Journal of Applied Physics, 1981. **52**: p. 1056-1065.
26. Campbell, J.A. and R.C. Waag, *Normalization of ultrasonic scattering measurements to obtain average differential scattering cross-sections for tissues.* Journal of the Acoustical Society of America, 1983. **74**: p. 393-399.
27. Madsen, E.L., M.F. Insana, and J.A. Zagzebski, *Method of data reduction for accurate determination of acoustic backscatter coefficients.* Journal of the Acoustical Society of America, 1984. **76**: p. 913-923.
28. Wear, K.A., et al., *Differentiation between acutely ischemic myocardium and zones of completed infarction in dogs on the basis of frequency-dependent backscatter.* Journal of the Acoustical Society of America, 1989. **85**: p. 2634-2641.
29. Chen, X., et al., *The Measurement of Backscatter Coefficient from a Broadband Pulse-Echo System: A New Formulation.* Ieee Transactions on Ultrasonics Ferroelectrics and Frequency Control, 1997. **44**: p. 515-525.
30. Hughes, M.S., et al., *Behavior of Resonant Peak of Attenuation of Albunex at Varying Power Levels and Durations.* Ultrasonic Imaging, 1998. **20**.
31. DeJong, N., *Ultrasound scattering properties of Albunex.* Ultrasonics, 1992. **31**: p. 175-181.
32. Lindner, J., et al., *Ultrasound Assessment of Inflammation and Renal Tissue Injury With Microbubbles Targeted to P-Selectin*, in *Circulation*. 2001. p. 2107-2112.
33. Christiansen, J., et al., *Noninvasive Imaging of Myocardial Reperfusion Injury Using Leukocyte-Targeted Contrast Echocardiography*, in *Circulation*. 2002. p. 1764-1767.
34. Leong-Poi, H., et al., *Noninvasive Assessment of Angiogenesis by Ultrasound and Microbubbles Targeted to α_v-Integrins*, in *Circulation*. 2003. p. 1-6.
35. Ishimaru, A., *Wave Propagation and Scattering in Random Media.* Vol. 1. 1978, New York: Academic Press.
36. Morse, P.M. and K.U. Ingard, *Theoretical Acoustics*. 1968, Princeton, NJ: Princeton University Press.

Table I

Property	Optison	Liquid-PFOB Nanoparticles
Resonant Peak	Yes	No
Exposure time dependence	Yes	No
Ambient Pressure Dependence	Yes	No
Ambient Temperature Dependence	Yes	No
Insonifying Power Dependence	Yes	No

Table IA. A comparison of the attenuation coefficient properties of the microbubble-based agent Optison and liquid perfluorocarbon nanoparticles. The nanoparticles attenuation is completely devoid of behavior required for microbubble like scattering.

Property (at 60 min. equilibrium)	Whole Porcine Blood	Porcine Plasma
Attenuation	Same as blood alone and independent of concentration	Same as plasma alone and independent of concentration
Backscatter	Same as blood alone and independent of concentration	~35 dB less than whole blood alone, Up to 15 dB greater than that of plasma alone and independent of concentration

Table IB . A comparison of the backscatter (not compensated for attenuation) properties liquid perfluorocarbon nanoparticles suspended in either whole porcine blood or porcine plasma. All comparisons are made at a time 60 minutes post-mixing so that upper bounds on measured quantities are obtained. In whole blood the nanoparticle backscatter is indistinguishable from that of whole blood alone. In plasma the backscatter in roughly 35 dB below that of whole blood .

Figure Captions

Figure 1. A) The architecture of the nanoparticle showing the thin stabilizing lipid layer surrounding the perfluorocarbon interior. B) An electron micrograph showing nanoparticles attached to fibrin strands surrounding a red blood cell. The nanoparticles are spherical as indicated in part A.

Figure 2. The experimental apparatus used to test the hypothesis that microbubble formation might be the basis for *in vivo* backscatter. Configuration **A** was used to generate pure unipolar pulses using step function excitation of the transducer. Configuration **B** was used instead of **A** to generate the pulse shown in Figure 5: a Doppler-like heating pulse preceding two unipolar pulses. Inset: the specimen chamber used for broadband attenuation measurements at different ambient pressures and temperatures

Figure 3. On the right the apparatus used to acquire data for this study. On the left specimen chamber used for low concentration measurements of attenuation and backscatter of nanoparticle suspensions in either whole porcine blood or plasma.

Figure 4. First row: effect of ambient pressure (0, 100, and 200 mm Hg, shown in separate panels) and exposure time (2, 20, 40, and 80 s, represented as four curves in each panel) for microbubble agent Optison, measured at 37 C with insonifying peak acoustic pressure of 0.65 MPa. The attenuation coefficient is clearly peaked between 1-2 MHz.

Peak height, width and location vary with exposure time, probably due to microbubble destruction and gas exchange. Second row: attenuation coefficient for liquid nanoparticle emulsion under similar experimental conditions; note complete lack of peak in attenuation. Third row: attenuation coefficient of emulsion under similar conditions as second row, but with higher peak acoustic pressure level (3.0 MPa). Fourth row: attenuation coefficient of emulsion under similar conditions as third row, but maintained at elevated ambient temperature of 46 C. All data were acquired using unipolar pulses generated by the apparatus shown in Figure 1A.

Figure 5. Panel A: the pulse used to simulate effects of clinical imager in Doppler-mode. Panel B: the resulting attenuation coefficient for nanoparticle emulsion. Panel C: the resulting attenuation coefficient for Optison. There is no evidence of exposure-time variation nor is there evidence of a microbubble-like resonant peak in the frequency range of the measurement. All data were acquired using unipolar pulses generated by the apparatus shown in Figure 1B.

Figure 6. Top Panel- a comparison of attenuation coefficients of PFOB based nanoparticles obtained in plasma (right side) and in whole blood (left side). Bottom Panel- a comparison of apparent backscatter coefficients obtained in plasma (right side) and in whole blood (left side). All data were acquired using unipolar pulses generated by the apparatus shown in Figure 1A. 0dB corresponds to the echo intensity of the flat reflector

1. Lanza, G.M., et al., *Molecular imaging of stretch-induced tissue factor expression in carotid arteries with intravascular ultrasound.* Investigative Radiology, 2000. **35**(4): p. 227-234.
2. Lanza, G.M., et al., *High-frequency ultrasonic detection of thrombi with a targeted contrast system.* Ultrasound in Medicine and Biology, 1997. **23**(6): p. 863-870.
3. de Jong, N. and F.J.T. Cate, *New ultrasound contrast agents and technological innovations*, in *Ultrasonics*. 1996. p. 587-590.
4. Lanza, G., et al., *In Vitro Characterization of a Novel, Tissue-Targeted Ultrasonic Contrast System with Acoustic Microscopy*, in *Journal of the Acoustical Society of America*. 1998. p. 3665-3672.
5. Unger, E.C., et al., *In vitro studies of a new thrombus-specific ultrasound contrast agent*, in *The American Journal of Cardiology*. 1998. p. 58G-61G.
6. Cotter B., K.O.L., Kimura B., Leese P., Quay S., Worah D., Demaria A.N.,, *Evaluation of the efficacy, safety and pharmacokinetics of QW3600 (Echogen) in man.* Circulation, 1994. **90**(4): p. 555-555 part 2.
7. Lanza, G. and S. Wickline, *Targeted Ultrasonic Contrast Agents for Molecular Imaging and Therapy*, in *Progress in Cardiovascular Diseases*. 2001. p. 13-31.
8. Lanza, G., et al., *Molecular imaging of stretch-induced tissue factor in carotid arteries with ligand-targeted nanoparticles*, in *Investigative Radiology*. 2000. p. 227-234.
9. Lanza, G., et al., *In vivo molecular imaging of stretch-induced tissue factor in carotid arteries with ligand targeted nanoparticles*, in *Journal of the American Society of Echocardiography*. 2000. p. 433-439.
10. Marsh, J.N., Hall, Christopher.S., Scott, Michael.J., Fuhrhop, Ralph.W., Gaffney, Paul.J., Wickline, Samuel.A., Lanza, Gregory.M., *Improvements in the ultrasonic contrast of targeted perfluorocarbon nanoparticles using an acoustic transmission line model.* IEEE Transactions on Ultrasonics Ferroelectrics and Frequency Control, 2002. **49**(1): p. 29-38.
11. Riess, J.G. and M.P. Krafft, *Fluorocarbons and fluorosurfactants for in vivo oxygen transport (blood substitutes), imaging and drug delivery.* MRS Bulletin, 1999. **24**: p. 42-48.
12. Riess, J.G., *fluorocarbon emulsions-Designing an Efficient Shuttle service for the Respiratory Gases - The So-called "Blood Substitutes"*, in *Fluorine Chemistry at the Millennium*, R.E. Banks, Editor. 2000, Elsevier Science: Oxford, UK. p. 385-431.
13. Hughes, M.S., et al. *Comparison of Ultrasound Scattering Behavior of Optison® and a Liquid Perfluorocarbon Nanoparticle Contrast Agent.* in *2002 IEEE Ultrasonics Symposium*. 2002: IEEE.
14. Hughes, M.S., et al. *Comparison of Ultrasound Scattering Behavior of Optison and a Liquid Perfluorocarbon Nanoparticle Contrast Agent.* in *142nd Meeting Acoustical Society Of America*. 2001. Fort Lauderdale FL: AIP.
15. Marsh, J.N., et al., *Broadband through-transmission signal loss measurments of Albunex suspensions at concentrations approaching in vivo doses.* Journal of the Acoustical Society of America, 1997. **101**(2): p. 1155-1161.

16. Yuan, K.K. and K.K. Shung, *Ultrasonic backscatter from flowing whole blood. I: Dependence on shear rate and hematocrit.* Journal of the Acoustical Society of America, 1988. **84**(52): p. 52-58.
17. Wang, S.-H. and K.K. Shung, *In vivo measurements of ultrasonic backscattering in blood.* IEEE Transactions on Ultrasonics Ferroelectrics and Frequency Control, 2001. **48**(2): p. 425-431.
18. Hall, C.S., et al., *Temperature dependence of ultrasonic enhancement with a site-targeted contrast agent.* Journal of the Acoustical Society of America, 2001. **110**(3): p. 1677-1684.
19. Hall, C.S., et al., *Time evolution of enhanced ultrasonic reflection using a fibrin-targeted nanoparticulate contrast agent.* Journal of the Acoustical Society of America, 2000. **108**(6): p. 3049-3057.
20. Ahmed, E., *Fractals and Chaos in Cancer Models.* International Journal of Theoretical Physics, 1993. **32**(2): p. 353-355.
21. Beier, J., et al., *Fractal surface analysis of pulmonary nodules based on high resolution computed tomography.* Rofo-Fortschritte Auf Dem Gebiet Der Rontgenstrahlen Und Der Bildgebenden Verfahren, 1997. **166**(4): p. 296-302.
22. Baish, J.W. and R.K. Jain, *Cancer, angiogenesis and fractals.* Nature Medicine, 1998. **4**(9): p. 984-984.
23. Baish, J.W. and R.K. Jain, *Fractals and cancer.* Cancer Research, 2000. **60**(14): p. 3683-3688.
24. Sigelmann, R.A. and J.M. Reid, *Analysis and measurement of ultrasound backscattering from an ensemble of scatterers excited by sine-wave bursts.* J. Acoust. Soc. Am., 1973. **53**: p. 1353-1355.
25. O'Donnell, M. and J.G. Miller, *Quantitative broadband ultrasonic backscatter: An approach to nondestructive evaluation in acoustically inhomogeneous materials.* Journal of Applied Physics, 1981. **52**: p. 1056-1065.
26. Campbell, J.A. and R.C. Waag, *Normalization of ultrasonic scattering measurements to obtain average differential scattering cross-sections for tissues.* Journal of the Acoustical Society of America, 1983. **74**: p. 393-399.
27. Madsen, E.L., M.F. Insana, and J.A. Zagzebski, *Method of data reduction for accurate determination of acoustic backscatter coefficients.* Journal of the Acoustical Society of America, 1984. **76**: p. 913-923.
28. Wear, K.A., et al., *Differentiation between acutely ischemic myocardium and zones of completed infarction in dogs on the basis of frequency-dependent backscatter.* Journal of the Acoustical Society of America, 1989. **85**: p. 2634-2641.
29. Chen, X., et al., *The Measurement of Backscatter Coefficient from a Broadband Pulse-Echo System: A New Formulation.* Ieee Transactions on Ultrasonics Ferroelectrics and Frequency Control, 1997. **44**: p. 515-525.
30. Hughes, M.S., et al., *Behavior of Resonant Peak of Attenuation of Albunex at Varying Power Levels and Durations.* Ultrasonic Imaging, 1998. **20**.
31. DeJong, N., *Ultrasound scattering properties of Albunex.* Ultrasonics, 1992. **31**: p. 175-181.

32. Lindner, J., et al., *Ultrasound Assessment of Inflammation and Renal Tissue Injury With Microbubbles Targeted to P-Selectin*, in *Circulation*. 2001. p. 2107-2112.
33. Christiansen, J., et al., *Noninvasive Imaging of Myocardial Reperfusion Injury Using Leukocyte-Targeted Contrast Echocardiography*, in *Circulation*. 2002. p. 1764-1767.
34. Leong-Poi, H., et al., *Noninvasive Assessment of Angiogenesis by Ultrasound and Microbubbles Targeted to α_v-Integrins*, in *Circulation*. 2003. p. 1-6.
35. Ishimaru, A., *Wave Propagation and Scattering in Random Media*. Vol. 1. 1978, New York: Academic Press.
36. Morse, P.M. and K.U. Ingard, *Theoretical Acoustics*. 1968, Princeton, NJ: Princeton University Press.

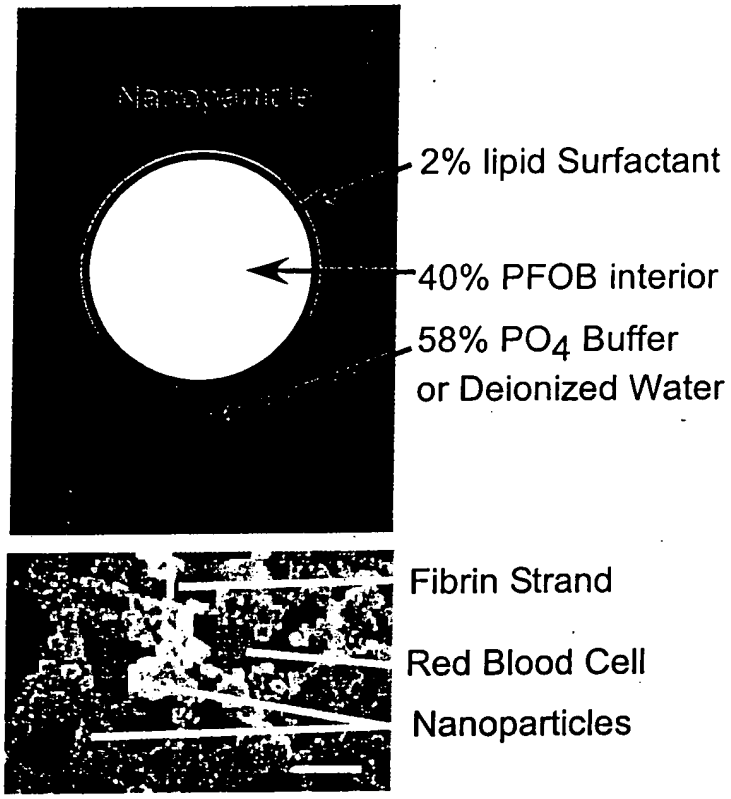
Nanoparticle
2% lipid Surfactant
40% PFOB interior
58% PO_4 Buffer
or Deionized Water
Fibrin Strand
Red Blood Cell
Nanoparticles
500 nm

Figure 1

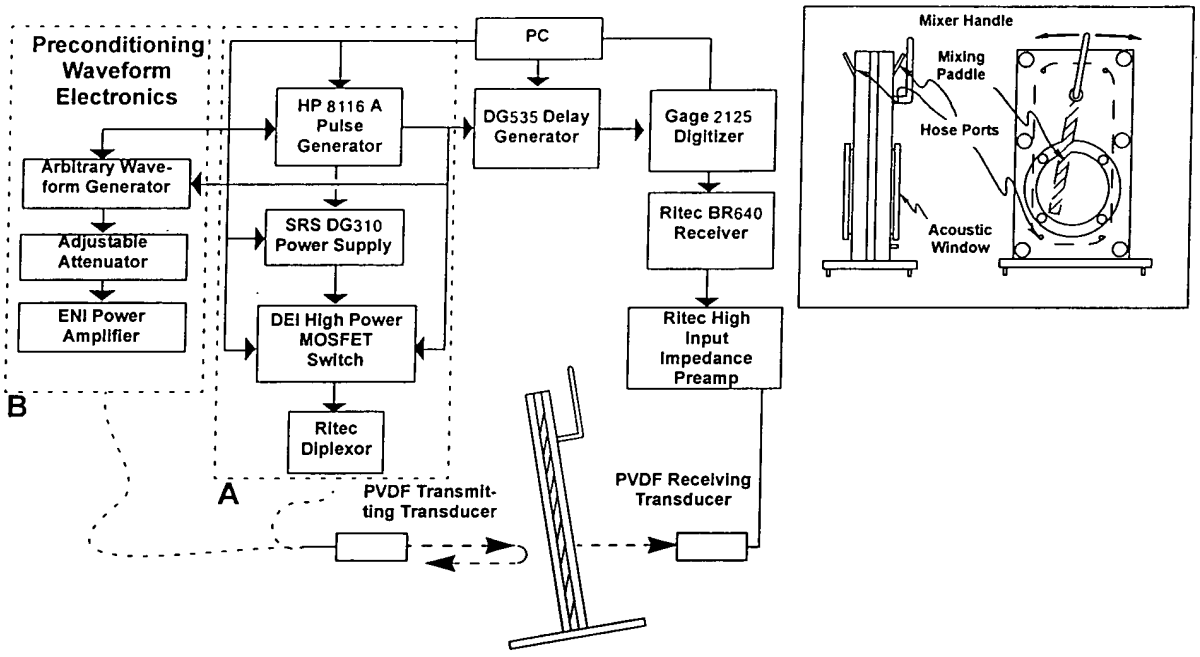
Preconditioning Waveform Electronics
Arbitrary Wave-form Generator
Adjustable Attenuator
ENI Power Amplifier
B
HP 8116 A Pulse Generator
SRS DG310 Power Supply
DEI High Power MOSFET Switch
Ritec Diplexor
A
PC
DG535 Delay Generator
Gage 2125 Digitizer
Ritec BR640 Receiver
Ritec High Input Impedance Preamp
PVDF Transmit-ting Transducer
PVDF Receiving Transducer
Mixer Handle
Mixing Paddle
Hose Ports
Acoustic Window

Figure 2

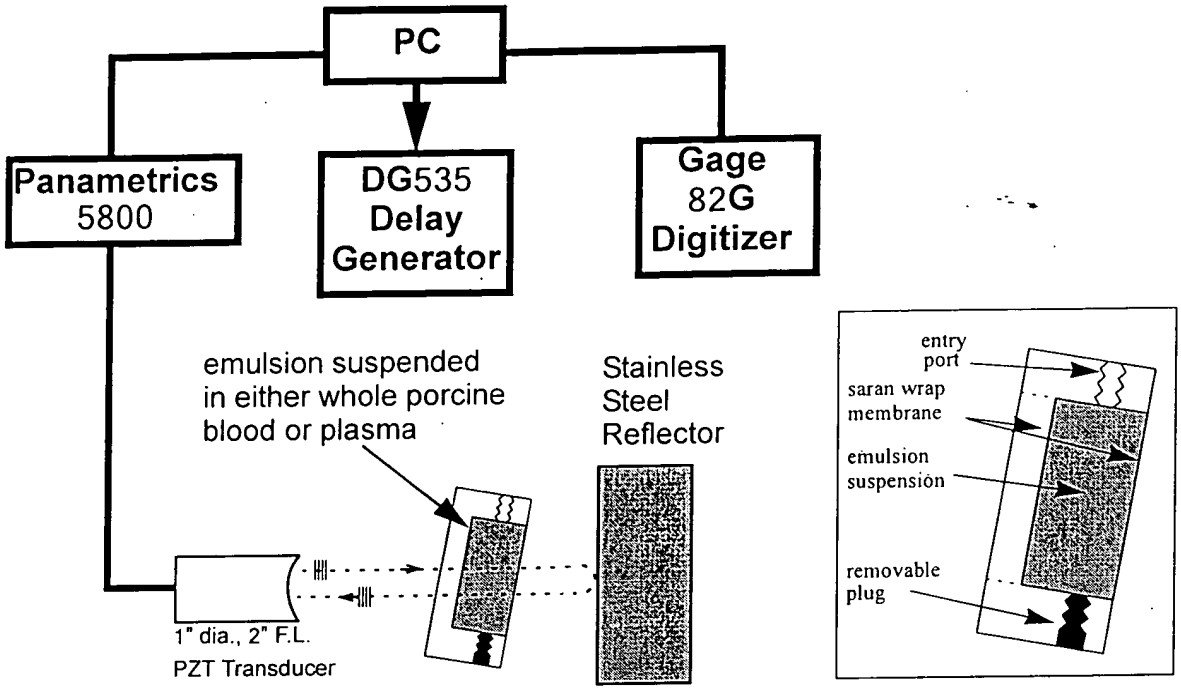
PC
Panametrics
5800
DG535
Delay
Generator
Gage
82G
Digitizer
emulsion suspended
in either whole porcine
blood or plasma
Stainless
Steel
Reflector
1" dia., 2" F.L.
PZT Transducer
entry
port
saran wrap
membrane
emulsion
suspension
removable
plug

Figure 3

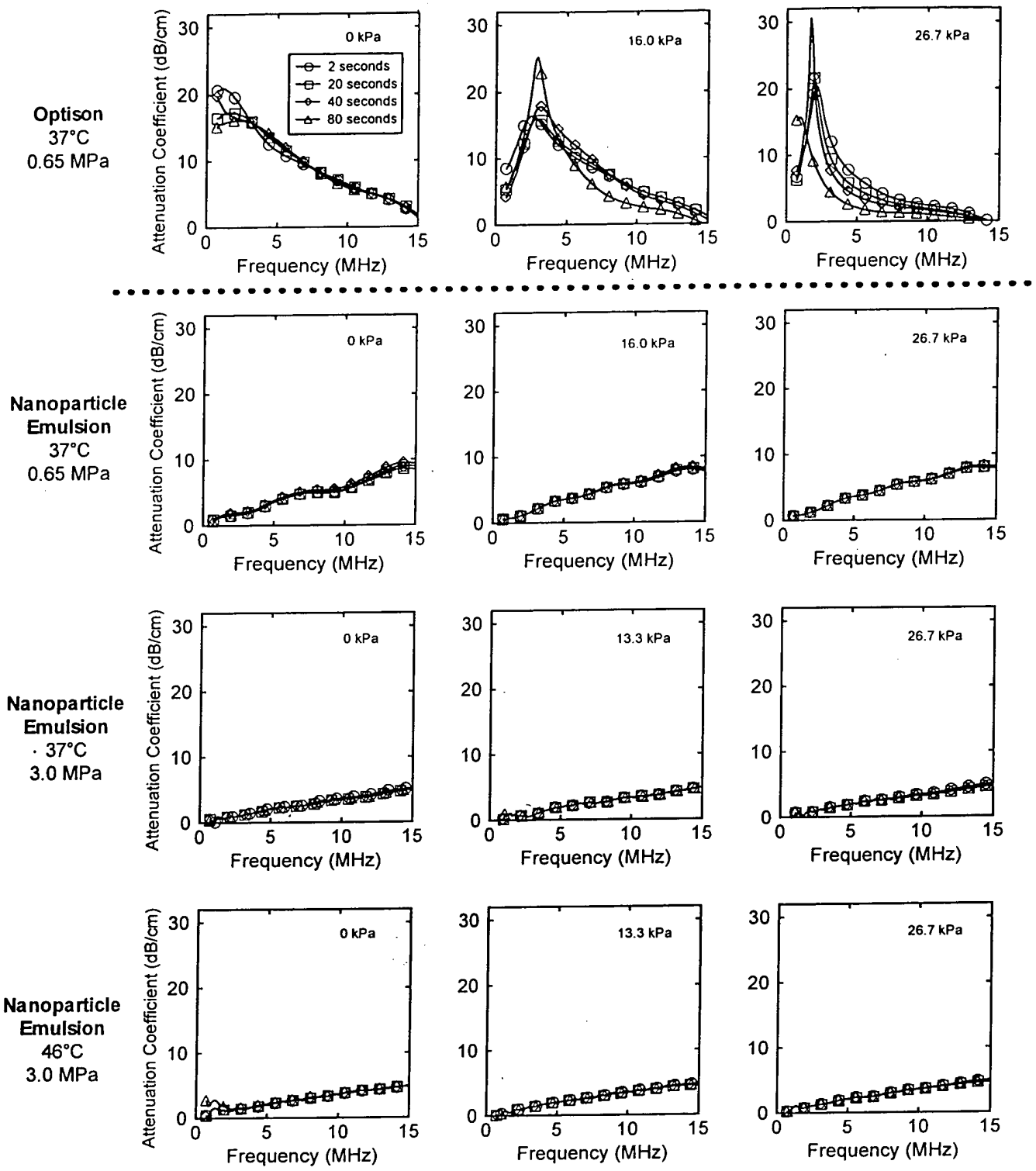
Optison
37°C
0.65 MPa
Nanoparticle Emulsion
37°C
0.65 MPa
Nanoparticle Emulsion
37°C
3.0 MPa
Nanoparticle Emulsion
46°C
3.0 MPa
Attenuation Coefficient (dB/cm)
Frequency (MHz)
0 kPa
16.0 kPa
26.7 kPa
13.3 kPa
2 seconds
20 seconds
40 seconds
80 seconds

Figure 4

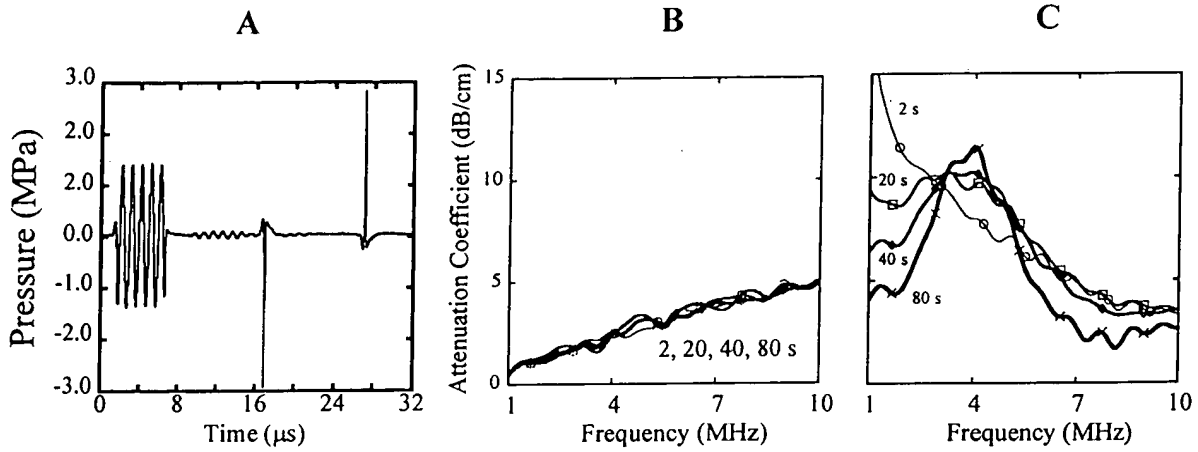
A
B
C
Pressure (MPa)
3.0
2.0
2.0
0.0
-1.0
-2.0
-3.0
0
8
16
24
32
Time (μs)
Attenuation Coefficient (dB/cm)
15
10
5
0
1
4
7
10
Frequency (MHz)
2, 20, 40, 80 s
2 s
20 s
40 s
80 s
1
4
7
10
Frequency (MHz)

Figure 5

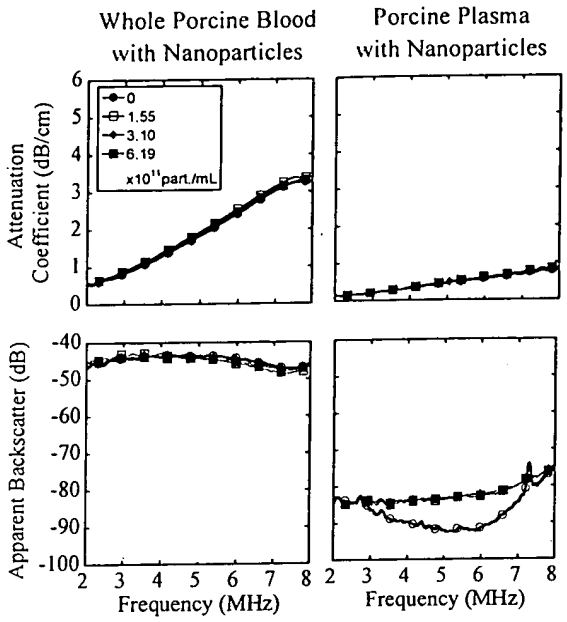
Whole Porcine Blood
with Nanoparticles
Porcine Plasma
with Nanoparticles
Attenuation
Coefficient (dB/cm)
0
1.55
3.10
6.19
x10^11 part./mL
Apparent Backscatter (dB)
Frequency (MHz)
Frequency (MHz)

Figure 6

REMARKS

Claims 1 and 18, the only independent claims, have been amended further to clarify that the nanoparticles used in the claimed methods are liquid and only liquid at all times during the claimed method. Applicants have made good faith efforts to propose claim language acceptable to the Office to establish what applicants have been trying to make clear during the prosecution – that the claims are directed to particles that are substantially free of any gas. This is done in order to distinguish the claimed methods from those involving compositions that depend for their efficacy on the presence of gas bubbles. Applicants cannot emphasize too strongly that the compositions useful in the claimed methods involve nanoparticles which do not contain any significant amount of gas. Applicants are at a loss to understand why a claim which consistently specifies "liquid nanoparticles" would be interpreted in any different way.

The amendment is submitted after final is thus simply for clarification. It does not constitute new matter or raise new issues because it does not change the intended scope of the claim at all. Entry of the amendment is thus respectfully requested.

Liquid Nanoparticles *vs.* Gas Microbubbles

The difference between the claimed liquid nanoparticles and gas microbubbles, such as those of the cited patent, are made evident in the results set forth in the enclosed manuscript, which includes the present inventors among the authors. The difference in behavior of these compositions is most apparent in Figure 4 which shows a comparison of the attenuation coefficient of Optison® (a microbubble-containing composition of gaseous fluorocarbon) as compared to the nanoparticle emulsions of the present application. As shown, the attenuation coefficient of liquid nanoparticles is essentially independent of temperature and emulsion pressure and changes only slowly and in a

predictable manner as a function of ultrasound frequency. The Optison® composition, on the other hand, shows dramatic differences as pressure is varied and dramatic differences as a function of frequency. The more consistent behavior of the claimed nanoparticle compositions is very advantageous in imaging studies, for example. Because of these consistent properties, the background generated by particles remaining in the bloodstream is less and clearly differentiated from the signal generated from the emulsion which is bound to a targeted tissue. This results in clearer images.

The Rejection Under 35 U.S.C. § 102(e)

All claims except claims 21, 73 and 75 were rejected as assertedly anticipated by Østenson, U.S. patent 6,375,931.

First, the Office asserts that performing ultrasound imaging procedures would inherently raise the local temperature citing Østenson at column 5, lines 5-46. Respectfully, there is no disclosure in the cited passage that has anything to do with either temperature or ultrasound. Lines 6-27 simply discuss the nature of possible phospholipids in the Østenson composition and lines 28-46 describe alternative encapsulation materials. Nothing is said about temperature or ultrasound. Thus, there is no basis for the conclusion drawn by the Office that ultrasound imaging begins at a lower temperature and ends at a higher temperature.

On this basis alone, the rejection may be withdrawn.

The Office next states that the nanoparticles of Østenson at the site "comprise" a liquid perfluorocarbon. That may be true; however, they are not "liquid nanoparticles." They must contain gas bubbles.